

Recovery of Electron-Irradiated Copper. I. Close Pair Recovery

J. W. CORBETT, R. B. SMITH,* AND R. M. WALKER
General Electric Research Laboratory, Schenectady, New York

(Received January 28, 1959)

Stage I recovery (14–65°K) of electron-irradiated, high-purity copper is shown to be composed of at least five substages: I_A , 14–24°K; I_B , 24–28.5°K; I_C , 28.5–33°K; I_D , 33–48°K and I_E , 48–65°K. I_A , I_B , and I_C recovery are discussed in further detail. (Discussion of I_D and I_E recovery is deferred to the following paper.) I_B and I_C are shown to have the characteristics of close-pair recovery. It is inferred that I_A also has these characteristics. The values of the activation energy for recovery are $E_A=0.05\pm 0.01$ ev, $E_B=0.085\pm 0.01$ ev, and $E_C=0.095\pm 0.01$ ev. An attempt to relate the observed close-pair spectrum to specific interstitial-vacancy configurations is described.

INTRODUCTION

THE recovery of the physical changes introduced by irradiation, cold-working, and quenching from an elevated temperature have qualitative similarities which suggest that the various treatments share common recovery processes.^{1,2} It is conventional to divide the recovery in copper into five stages characterized by the temperature range in which the recovery occurs³: Stage I, 14–65°K; II, 65–233°K; III, 233–373°K; IV, 373–473°K and V, $T>473$ °K. Although there is a considerable amount of experimental information available, there has been no general agreement between different investigators on the specific lattice defects and processes operative in each stage. Clearly the delineation of the recovery processes is basic to the understanding of the physical effects of the defects and of the processes by which the defects are introduced. One of the key points in the controversy surrounding the assignment of recovery processes to the various stages is whether Stage I recovery involves long distance, free-migration of a defect or involves only localized readjustments of the lattice. Several authors, adopting this latter point of view, have suggested that Stage I recovery is due to one, or both, of two processes: (1) the re-ordering of disturbed regions of the lattice which were initially disordered by displacement spikes⁴; and (2) the recombination of “close pairs”—i.e., interstitial-vacancy pairs with such a small (i-v)

separation that they effectively form a bound system due to their mutual interaction.

In the case of copper irradiated with ~ 1 -Mev electrons, it is expected that the amount of spike-type damage is negligible and only interstitials and vacancies should be produced. The question then is whether any or all of the Stage I recovery observed after such an irradiation is due to close pairs. In a previous paper⁵ we showed that this recovery could not be described by any single simple kinetic law.

Subsequently,^{6,7} it was shown that the Stage I recovery consisted of discrete substages. In electron-irradiated copper we observe at least five substages which we shall designate as I_A , I_B , I_C , I_D , and I_E in order of increasing temperature.

In the present paper we show that I_A , I_B , and I_C have the characteristics expected of close pair recovery. The possible origins of these close-pair species are discussed.

In the following paper I_D and I_E are discussed and shown to be associated with a defect which is capable of freely migrating through the lattice. Following Huntington's calculations,⁸ this defect is identified as an interstitial atom. The results of these papers are therefore incompatible with an assignment of all of Stage I recovery with purely localized defects.

EXPERIMENTAL

The experimental apparatus has already been described in detail,⁵ and only those features pertinent to the present work will be repeated here.

All the data presented in these two papers are resistivity data. The resistance measurements were made by the standard potentiometric technique. A Rubicon 6-Dial Thermofree Potentiometer and 300 ma measuring current were used. Careful shielding permitted measurement with a precision of $\pm 3\times 10^{-8}$ ohm corresponding to a resistivity uncertainty of $\pm 5\times 10^{-13}$ ohm cm.

* Now at Hanford Laboratory Operations, Hanford Atomic Products Operations, Richland, Washington.

¹ For recent reviews see Holmes, Corbett, Walker, Koehler, and Seitz, *Proceedings of the Second United Nations International Conference on Peaceful Uses of Atomic Energy, Geneva, 1958* (United Nations, Geneva, 1959), paper No. 2385; A. Seegar, paper No. 998; G. J. Dienes and G. H. Vineyard, *Radiation Effects in Solids* (Interscience Publishers, Inc., New York, 1957); F. Seitz and J. S. Koehler, in *Solid State Physics* (Academic Press, Inc., New York, 1956), Vol. 2, pp. 307–442.

² We do not wish to imply that the recovery in a given temperature range following different treatments is always due to identical recovery processes. This point will be developed in the following paper.

³ H. G. van Bueren, *Z. Metallk.* **46**, 272 (1955); thesis, Leiden, 1956 (unpublished); Philips Research Repts. **12**, 1, 190 (1957).

⁴ The possibility of this type of damage was first proposed by J. A. Brinkman, *J. Appl. Phys.* **25**, 961 (1954); *Am. J. Phys.* **24**, 246 (1956).

⁵ Corbett, Denney, Fiske, and Walker, *Phys. Rev.* **108**, 954 (1957).

⁶ Magnuson, Palmer, and Koehler, *Phys. Rev.* **109**, 1990 (1958).

⁷ J. W. Corbett and R. M. Walker, *Phys. Rev.* **110**, 767 (1958).

⁸ H. B. Huntington, *Phys. Rev.* **91**, 1092 (1953).

The source of high-energy electrons for the irradiations was a commercial model G. E. resonant transformer. The average electron energy incident on the sample for all the irradiations reported here was ~ 1.4 Mev. Most of the irradiations were performed with a current of $\sim 1 \mu\text{a}/\text{cm}^2$ incident on the sample. In the present experiments the accelerator was equipped with a 0.003-cm titanium window and hence had somewhat less energy spread than the previously reported experiments.

Special care was taken to obtain high-purity copper, and we feel this is an important feature of the present work. The starting material was American Smelting and Refining Company copper of 99.999% stated purity. This material was zone-refined (six passes) and then rolled through clean, dry, hardened, carbon-steel rolls to a thickness of 0.0032 cm. Frequently, between rolling passes, the foil was etched in dilute nitric acid and then carefully washed. Several pieces of the foil were then annealed *in vacuo* for $\frac{1}{2}$ hour at 450°C . These pieces of foil were then photoengraved to obtain, in each, a pattern of length-wise strips 0.75 mm wide. In the irradiations half of the foil is shielded from the beam and serves as a control. The residual resistivity of the foil material was 1.5×10^{-9} ohm-cm at 4.2°K . X-ray measurements showed an average grain size slightly larger than the foil thickness. There was no preferred orientation in the foils.

It was expected that the recovery studies could be influenced by impurities.⁹ Therefore, all the experiments which are employed in the detailed analysis of the recovery were performed on a single sample. To insure that successive experiments were essentially *ab initio* experiments and were equivalent, the sample was annealed *in situ* at 150°C for $\frac{1}{2}$ hour between experiments. While $\sim 0.1\%$ of the resistivity introduced by irradiation at 20°K remained after this anneal, no effect of this residue on the recovery studies was detected. Measurements made on the same zone-refined copper, but not the same specimen, exhibited the same recovery features.

It was also expected that the recovery might depend on the concentration of the defects. Consequently, unless this concentration dependence was actually sought in an experiment, the experiment was always carried out with a standard total electron flux—a standard defect concentration.

The best value for the resistivity associated with radiation induced defects now appears to be $\sim 3 \times 10^{-6}$ ohm cm per atomic percent of defects.^{6,10} We shall use this value to estimate the defect concentration corresponding to our resistivity data. The resistivity increment in the standard irradiation was 2.7×10^{-10}

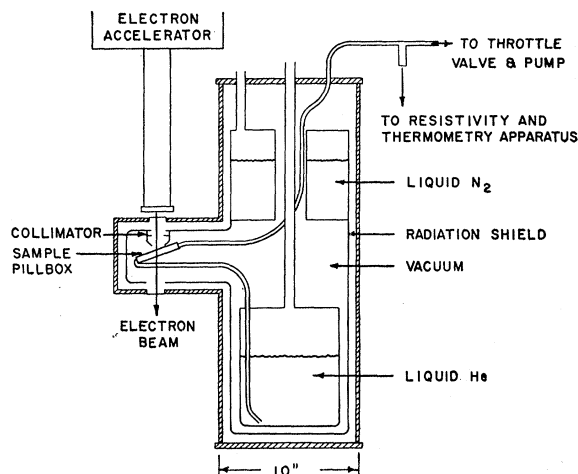


FIG. 1. Schematic drawing of electron-damage cryostat.

ohm cm, which is then 0.9×10^{-4} at. % or ~ 1 ppm at. conc.

We previously deduced a value of 1.5×10^{-6} ohm cm per atomic percent of radiation-induced defects,^{5,11} based on the dependence of the damage production rate on the bombarding electron energy. As we shall show in a future publication, the reconciliation of this number with the present 3.0×10^{-6} ohm cm/1 at.% resolves the discrepancies between theory and experiment for the production rate of damage by both electrons and deuterons, which lends further credence to this latter number.

A schematic diagram of the crystal is shown in Fig. 1. The foil was mounted in the pill-box assembly through which liquid refrigerant (helium or hydrogen) was pumped. The foil was supported only at the non-irradiated ends. The irradiated and control samples were side by side and the coolant flowed on all sides of the samples.

Although there were two carbon resistance thermometers and two thermocouples in the coolant stream, the temperature dependent resistivity of the control sample was used as the primary thermometer. The output of the sample-resistance potentiometer was fed into a Varian G-11 recorder, which was used to monitor and record the control sample resistance continuously. The control sample resistance readings were converted to a temperature scale in two ways. In previous publications we have fitted the temperature-dependent resistivity data to the Grüneisen theory at 273°K , 77.4°K and 20.4°K . In the present work we have used the resistivity *vs* temperature data of Magnuson *et al.*⁶ measured on a copper sample with about the same residual resistivity as ours. While we feel that this latter temperature scale is more accurate, there is no essential difference between the results of

⁹ Blewitt, Coltman, Klabunde, and Noggle, *J. Appl. Phys.* **28**, 639 (1957).

¹⁰ R. O. Simmons and R. W. Balluffi, *Phys. Rev.* **109**, 335 (1958); R. W. Vook and C. A. Wert, *Phys. Rev.* **109**, 1529 (1958).

¹¹ A. E. Fein, *Phys. Rev.* **109**, 1076 (1958).

the recovery analysis (e.g., energetics or kinetics) for the two scales.

The sample temperature was regulated by jointly controlling the amount of refrigerant pumped past the sample and the power applied to the heaters wound on the pillbox and on the refrigerant inlet line. This temperature control arrangement was quite versatile. It allowed us to make resistivity measurements at the refrigerant temperature, thereby ensuring maximum sensitivity; to irradiate at a low temperature or a high temperature (80°K); to carry out recovery studies with isothermal or isochronal pulse-annealing schedules; and, finally, to perform combinations of these irradiations and recovery studies *with no intervening high temperature (>80°K) annealing*. In the isothermal experiments the specimen temperature was pulsed to the annealing temperature for a series of increasing time increments. In the isochronal experiments the specimen temperature was pulsed to successively higher temperatures for the same length of time—ten minutes. It took a maximum of two minutes total elapsed time to reach any annealing temperature below 80°K. The control sample temperature (resistance) was continuously recorded during the pulse. The rise-time portion of the time-temperature curve of each pulse was numerically integrated using $\exp(-Q/kT)$ as a weight function to give the equivalent time at temperature. The activation energy initially used in the Boltzmann factor was determined by analyzing the data without the rise time correction. In practice the rise times corresponded to an equivalent time at temperature of ~ 0.3 min. This number is sufficiently small that the first correction for rise time is accurate enough. The effect of including the rise time correction on the calculation of activation energy is significant, however, and all the data quoted in these papers include this correction unless otherwise noted. The maximum temperature fluctuation during the annealing at the final temperature was $\pm 0.1^\circ\text{K}$.

Although in some experiments in this series liquid helium was used as the refrigerant, in most of the experiments liquid hydrogen was used. In the case of our preliminary recovery experiments⁵ liquid helium was used, but contrary to what was reported, the sample temperature in those measurements was probably not always below 12°K. During some of those irradiations the sample temperature was apparently sufficiently high that I_A recovery proceeded during irradiation, and this recovery was not observed. In the present experiments the electron flux was lowered until the fractional amount of recovery in I_A remained constant with decreasing current density. Because I_A comprises such a small fraction of the damage the conclusions made previously⁵ concerning the energy dependence of the damage production rate and the recovery of the damage, are not vitiated by the omission of I_A . Measurements of the recovery as a function of electron current density during irradiation

with liquid hydrogen refrigerant indicated that none of the I_B recovery was taking place during irradiation.

An experiment was done to ensure that the character of I_B , I_C , I_D , and I_E recovery was the same if either liquid helium or liquid hydrogen were used as the refrigerant. Of course, when liquid hydrogen is used I_A is not observed. However, liquid hydrogen is far more convenient for us to use than liquid helium. Consequently, most of the detailed measurements have been done on I_B , I_C , I_D , and I_E produced by irradiating at liquid hydrogen temperature.

The use of liquid hydrogen as a refrigerant has the possible complication that resistivity changes measured at the hydrogen boiling point may be due in part to changes in the temperature dependent part of the resistivity. However, consideration of the data available on the change in the temperature dependent resistivity due to irradiation^{6,12} shows that for the total defect concentrations used in the present work this effect is not significant.

Because of the inherent experimental limitations of the apparatus (e.g., sample temperature fluctuation, measuring apparatus limitations, etc.) the general reproducibility of the recovery data presented in these papers is $\sim \pm 0.3\%$ of initial resistivity increment.

ANALYSIS

We shall briefly review the basic concepts of the radiation damage process in order to establish a frame work for discussing the recovery. We have previously shown⁵ that a bombarding electron must transmit on the average, an energy of ~ 22 ev to a struck atom in order to produce a lattice defect. In the case of our 1.4-Mev electron irradiations the maximum energy (T_m) that can be imparted to the lattice atom is 115 ev. The average energy imparted to the lattice atom, considering collisions which impart between 22 and 115 ev, is 39 ev. We see then that on the average, the recoiling lattice atom does not have the necessary 22 ev to produce another defect in a collision with another lattice atom. In this case we expect a particularly simple kind of damage—an interstitial-vacancy pair, or Frenkel pair. Since electron-atom collisions which transfer the required 22 ev are relatively rare, the interstitial-vacancy pairs will be distributed randomly throughout the sample. Further, since the sample thickness is a small fraction of range of the bombarding electrons the i-v pairs will be distributed homogeneously through the sample.

Since T_m is 115 ev, we might expect some multiple defect production to be possible. The theory of defect production should be useful in assessing the extent of multiple defect production. However, this theory predicts values of defect concentration much higher than the concentrations deduced from experiment using the value of resistivity increment per atomic

¹² D. Bowen and G. W. Rodeback, *Acta Met.* 1, 649 (1953).

percent of defects suggested by the measurements of the density change.^{6,10} The discrepancy is about a factor of 2 for electron irradiations and $\sim 6-7$ for heavy-particle irradiations. As we will discuss in a future publication, a simple and reasonable modification of the defect production theory helps resolve these discrepancies. It suffices here to observe that this modification is in the direction of reducing the number of multiple defects to the point that in the electron irradiations we may ignore them. In the recovery analysis presented in the present papers we will therefore assume that all of the defects are produced in the form of isolated Frenkel pairs.

The interstitial-vacancy separation in each of the Frenkel pairs can vary, depending on the energy transferred in the production collision and the crystallographic direction of the recoiling interstitial. If the interstitial comes to rest near a vacancy, the interaction between the defects can make the activation energy to jump in the direction of the vacancy less than the energy to jump away. As the temperature of the sample is raised these "close pairs" will recombine preferentially. If there are several close pair species the type with the lowest activation energy will go first, and so on. The interstitials which are sufficiently far removed from a vacancy will not move until a temperature is reached at which free migration through the lattice occurs. The freely migrating interstitial performs a random-walk motion and recombines with its own vacancy or another depending on the distribution of the defects in the lattice. The freely migrating interstitial may partake in a variety of interactions besides annihilation, and the description of the recovery process becomes quite complicated. In the present paper we shall be concerned only with the close pairs.

Close pair recovery is a purely localized interaction and should be quite insensitive to the presence of other defects in the crystal. This recovery is described by a simple monomolecular rate equation:

$$dC/dt = -CA \exp(-E_m/kT), \quad (1)$$

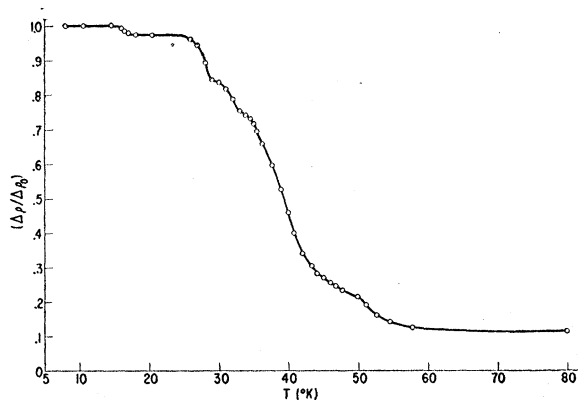


FIG. 2. Isochronal recovery curve. $(\Delta\rho_0) \sim 2.7 \times 10^{-10}$ ohm cm, or an initial defect concentration of ~ 1 ppm (see text).

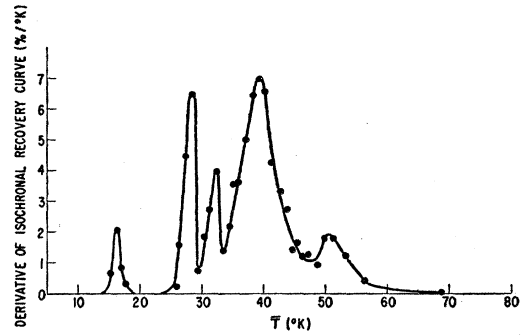


FIG. 3. Numerical derivative of the isochronal recovery curve shown in Fig. 2.

where C is the concentration of close pairs, E_m is the activation energy for a jump, and A is termed the frequency factor. For a constant temperature, integration of Eq. (1) gives

$$C/C_0 = \exp[-tA \exp(-E_m/kT)]. \quad (2)$$

Assuming that the resistivity ρ is proportional to C , a plot of $\ln[\rho(t)/\rho_0]$ vs t should give a straight line.

If there are several close pair species with differing activation energies and values of A , then we shall have a sum of equations like Eq. (2). In our case the activation energies of the species differ sufficiently that we can use the isothermals to resolve the species and to evaluate the corresponding activation energy and value of A .

Clearly the test of fitting the recovery curves to Eq. (2) requires of the experiment only that the precision in resetting to a particular temperature be good. Determination of the value of E_m , however, involves precise knowledge of the absolute value of the temperature and, in our experiments, is subject to more error.

RESULTS

General Features of Stage I Recovery

Figure 2 shows the results of a Stage I isochronal annealing experiment in which the defect concentration was 9×10^{-7} at. conc. Figure 3 presents a simple numerical derivative with respect to temperature of this isochronal. As can be seen there are five distinct substages of recovery, or *peaks*. This peak structure is quite reproducible and represents at least five recovery processes which differ quantitatively from each other. As we shall see there are also qualitative differences between these recovery processes. The possibility exists that with higher resolution and accuracy further substages might be detected, although all our recovery data are accounted for by five recovery processes.

That this structure is a genuine feature of the recovery and is not connected with uncertainties in the temperature scale can be demonstrated in two ways. Firstly, for the structure to represent uncertainties in

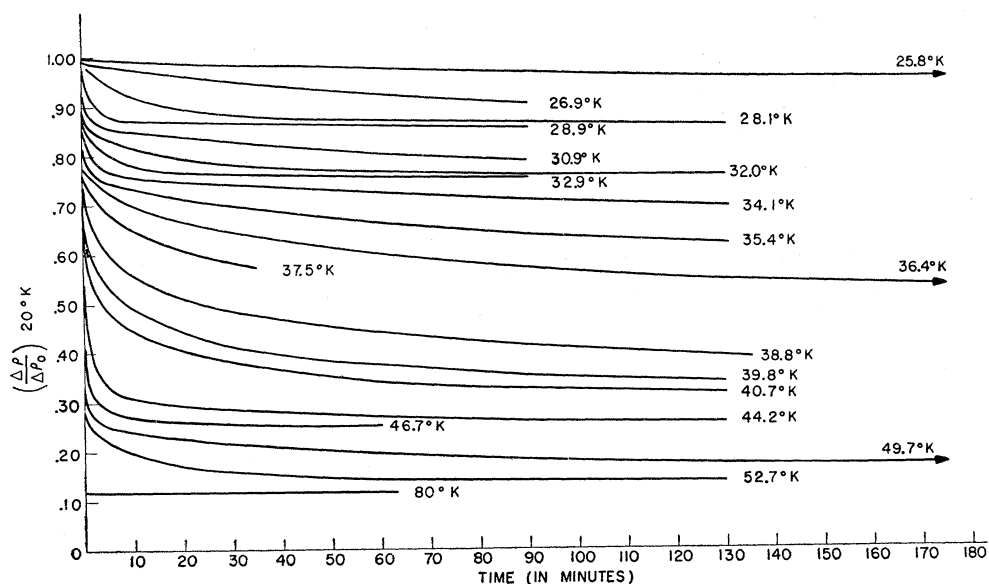


FIG. 4. Isothermal recovery curves. Each curve represents an independent experiment. All the irradiations for these recovery curves were performed at 20.4°K to a total radiation-induced resistivity increment of 2.7×10^{-10} ohm cm, or ~ 1 ppm defect concentration (see text).

the temperature scale would require the temperature dependent resistivity to exhibit this structure, which it does not. Secondly, and conclusively, we may consider the results of a series of independent isothermal recovery experiments. For a single recovery process, the isothermal recovery rate after, say, ten minutes will depend on the temperature at which the isothermal is carried out. Clearly, this rate will be zero if the temperature is so low no recovery is occurring. The rate at ten minutes will also be zero for an isothermal at a temperature where the recovery is completed in less than ten minutes. For isothermals at intermediate temperatures the rate will first increase to a maximum value and then decrease. However, if several recovery processes are occurring in sequence, we would expect this rate to go through several maxima and minima. In such a series of isothermals the only requirement of the temperature scale is that we can tell if one temperature is higher than another. We have performed such a series of isothermals for the temperature range of 20–80°K, regarding the separation of the recovery peak at 16°K from that at 27°K as manifestly real. These isothermals are shown in Fig. 4 and show saturation

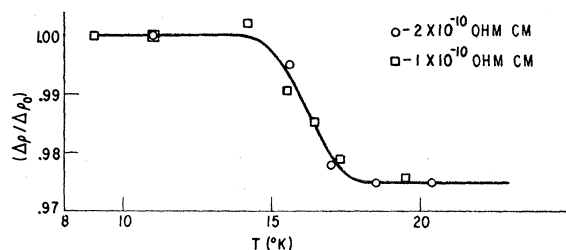


FIG. 5. Isochronal recovery curve for I_A recovery.

levels corresponding to the isochronal structure. Indeed it is possible analytically to predict the isochronal curves from the energetics and kinetics information obtained from the isothermals.

We shall designate the recovery substages as I_A, \dots, I_E in order of increasing temperature: $I_A, 14\text{--}24^\circ\text{K}$; $I_B, 24\text{--}28.5^\circ\text{K}$; $I_C, 28.5\text{--}33^\circ\text{K}$; $I_D, 33\text{--}48^\circ\text{K}$ and $I_E, 48\text{--}65^\circ\text{K}$. In present case (1.4-Mev bombarding electron energy) these substages contain the following percentages of the *total recovery*: $I_A\text{--}2.5\%$, $I_B\text{--}13.1\%$, $I_C\text{--}10.0\%$, $I_D\text{--}48.8\%$ and $I_E\text{--}12.8\%$; (II+III+IV+V)—12.8%, all percentages being to within $\frac{1}{2}\%$. In the following paper we shall show that both I_D and I_E recovery are associated with free interstitial migration. In the present paper we shall discuss only $I_A, I_B,$ and I_C recovery.

The results of two isochronal annealing experiments on I_A recovery are shown in Fig. 5. These two experiments were performed with bombarding electron fluxes differing by a factor of five. The fact that the same amount of I_A recovery is observed in both experiments demonstrates that the beam heating was not sufficient to cause any I_A recovery during irradiation. Although the defect concentration was slightly different in these runs, we do not regard this as conclusive proof of concentration independence of this recovery. Because I_A recovery is so small and because it requires liquid helium as a refrigerant we have not made detailed studies of this substage. Rather, the nature of I_A recovery is inferred from the nature of I_B and I_C . Consequently, we shall defer further discussion of I_A until I_B and I_C have been discussed.

In Fig. 6 are shown the results of three isochronal annealing experiments performed on I_B and I_C recovery

at different defect concentrations: 1.0×10^{-6} , 6.0×10^{-6} , and 1.8×10^{-5} atomic conc. We see that I_B and I_C recovery are concentration independent.

The isothermal annealing experiments performed on I_B and I_C recovery are shown in Fig. 7. In comparing the resistivity values to Eq. (2) it is necessary to ascertain the amount of recovery to be ascribed to the various substages; that is, to subtract the resistivity at which the next stage becomes operative. The value to be subtracted was found by trial and error in order to give the best fit to Eq. (2). Of course, the same value was subtracted for all the isothermals of a given substage.

Substage I_B

The results of the analysis of the I_B isothermals are presented in Fig. 8. The activation energy which is

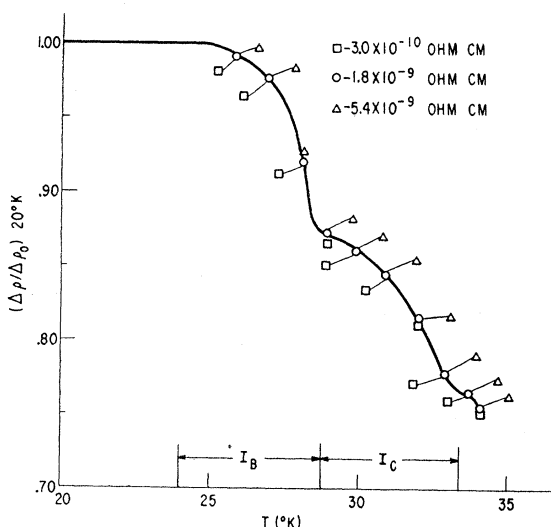


FIG. 6. Concentration dependence of the isochronal annealing of I_B and I_C recovery. The recovery is normalized at 20.4°K . As discussed in the text, the initial defect concentrations corresponding to these curves are 1.0×10^{-6} , 6.0×10^{-6} , and 1.8×10^{-5} , respectively.

obtained is $E_B = 0.085 \pm 0.01$ ev. The value of the frequency factor A is $8 \times 10^{11} \text{ sec}^{-1}$ to within a factor of five. To arrive at a theoretical value of A would involve detailed knowledge of the defect configuration, which we do not yet possess. We may estimate A , however, by neglecting the entropy contributions to the kinetics and saying¹³ $A \approx kT/h$, from which we obtain $A \sim 6 \times 10^{11} \text{ sec}^{-1}$. We consider this agreement quite satisfactory.

Substage I_C

The results of the analysis of the I_C isothermals are presented in Fig. 9. The activation energy is $E_C = 0.095 \pm 0.01$ ev. The value of A is again $8 \times 10^{11} \text{ sec}^{-1}$ to within a factor of five.

¹³ See Glasstone, Laidler, and Eyring, *The Theory of Rate Processes* (McGraw-Hill Book Company, New York, 1941).

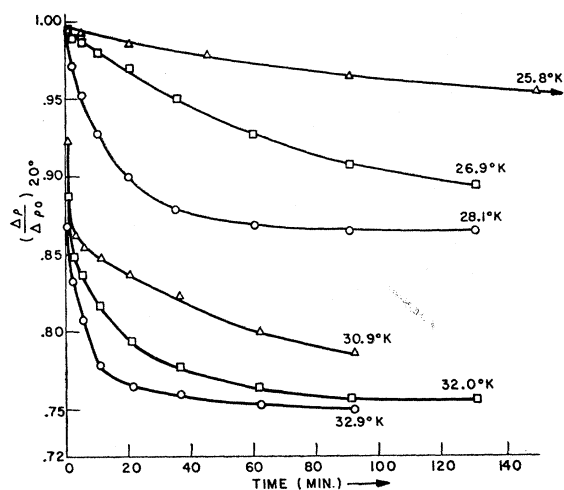


FIG. 7. I_B and I_C isothermal recovery curves. These curves are normalized at 20°K , and were all performed with an initial defect concentration $\sim 9 \times 10^{-7}$.

As can be seen from the figures the I_B and I_C recovery obey Eq. (2) quite satisfactorily with a reasonable frequency factor. These pieces of evidence form the basis for assigning I_B , I_C , and by inference, I_A recovery to "close pairs."

Substage I_A

We assume that I_A recovery involves the same frequency factor as I_B and I_C . The ratio of the activation energy to the temperature at which one-half the recovery of the substage is completed, is then a convenient scale factor for estimating the activation energy of the I_A recovery. In this manner we arrive at $E_A = 0.05 \pm 0.01$ ev.

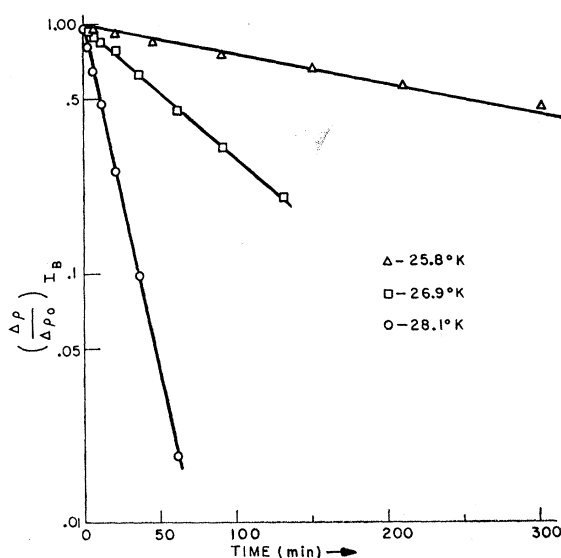


FIG. 8. I_B isothermal recovery curves on a first order plot. The data are those shown in Fig. 7.

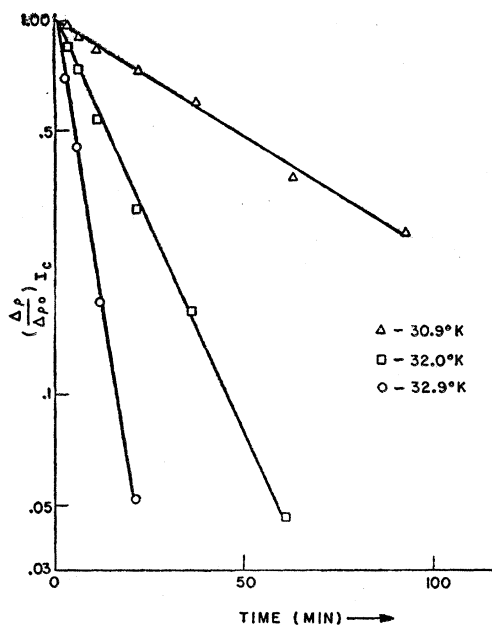


FIG. 9. I_C isothermal recovery curves on a first order plot. The data are those shown in Fig. 7.

DISCUSSION

Although the data show all the features expected of close pair recovery and are so interpreted, there remains the possibility that the results can be accounted for in a different way. Specifically, if the interstitials were freely moving they could be trapped at defects in the crystal other than the radiation-induced vacancies. If the concentration of trapping sites greatly exceeded the concentration of vacancies we would again expect, as has been shown by Waite,¹⁴ an equation like Eqs. (2). Different species of trapping sites with different binding energies could give discrete stages in the recovery. However, in order to account for the results the concentration of such trapping sites would have to be greatly in excess of either the number of chemical impurities or dislocation sites expected in this pure, annealed material. Further, in the next paper we show directly that trapping sites do not dominate the recovery in substage I_B . The trapping sites would therefore have to have low binding energies exclusively.

Perhaps the strongest evidence, however, that these peaks are intrinsic and hence due to close pairs is to be found in the comparison of the present experiments with those previously reported using deuterons. Magnuson, Palmer, and Koehler⁶ have presented the results of an experiment which consisted of a series of sequential isothermal annealing experiments on Stage I recovery produced by bombarding copper with 10-Mev deuterons. Analyzing their data, they obtain four discrete recovery stages for Stage I recovery. Well within the experimental limits of both experiments

their first three stages correspond, in both activation energy and frequency factor, to the stages we have labeled I_A , I_B , and I_C . Their fourth stage corresponds to our I_D plus I_E , as discussed in the next paper. They assigned their first three stages to close pair recovery, basing their argument on the fact that the calculated number of jumps to annihilation is small. Further, their experiment was performed with the radiation-induced defect concentration $\sim 2 \times 10^{-4}$ at. conc., which was higher than expected impurity concentration thereby ruling out impurity effects.

It is interesting to note that the relative population of the various substages of Stage I in the deuteron results is almost the same as in the electron recovery. In a subsequent publication we shall discuss the behavior of the recovery as a function of incident electron energy. We simply observe here that there is a small shift in the populations of the various substages with decreasing electron energy. This is what one would anticipate for close pairs but not for impurity effects.

In toto then, we believe these facts show that the discrete recovery spectrum is intrinsic and that I_A , I_B , and I_C are due to the recovery of different close-pair species.

We now consider the problem of identifying the specific configurations of interstitial and vacancy responsible for the substages I_A , I_B , and I_C . Figure 10 shows the face-centered cubic copper lattice with an interstitial assumed to reside in the body-centered position. We have shown only atoms which are crystallographically nonequivalent and have labeled them with increasing distance from the interstitial. In Table I we present the direction cosines, distances, and occupation numbers for a number of possible vacancy positions.

TABLE I. Direction cosines, distances, and occupation numbers for a number of possible vacancy positions. N designates the number of the lattice site, labeled with increasing distance from the interstitial site (see Fig. 10). r is the distance of the lattice site from the interstitial expressed in units of one half the lattice parameter. S is the number of equivalent sites. l , m , n are the direction cosines with respect to the cubic axes of the vector connecting the interstitial and the lattice site. A permutation of the direction cosines in the table will delineate the lattice sites shown in Fig. 10. $\Gamma = 0.400 - 2(l^2m^2 + m^2n^2 + n^2l^2)$.

N	r^2	S	lr	mr	nr	Γ
1	1	6	1	0	0	+0.400
2	3	8	1	1	1	-0.267
3	5	24	1	2	0	+0.080
4A	9	6	1	0	0	+0.400
4B	9	24	1	2	2	-0.192
5	11	24	1	1	3	+0.086
6	13	24	2	3	0	-0.026
7A	17	24	1	4	0	+0.290
7B	17	24	2	2	3	-0.210
8	19	24	1	3	3	-0.148
9	21	24	1	2	4	+0.018
10A	25	6	1	0	0	+0.400
10B	25	16	3	4	0	-0.060
11A	27	24	1	1	5	+0.260
11B	27	8	3	3	3	-0.267
12A	29	24	2	5	0	+0.162
12B	29	48	2	3	4	-0.180

¹⁴ T. R. Waite, Phys. Rev. **107**, 463, 471 (1957).

The only calculation we are aware of that has sought to calculate the stability of close i-v pairs has been performed by Tewordt.¹⁵ He concluded that the configuration with a vacancy in site 3 is unstable. No conclusions were reached for any of the other configurations. Since a vacancy in site 1 is certainly unstable, this leaves sites 2, 4, ... as possible stable vacancy positions. Theoretically⁸ it is not certain that the stable interstitial position is as assumed above and certainly more detailed calculations need to be performed on this whole problem.

In the absence of any detailed calculation we now inquire what elasticity theory can say on the matter. Eshelby¹⁶ has treated the elastic interaction between point defects with cubic symmetry and gives for the interaction energy between a pair of defects which produce volume changes in the medium of ΔV_1 and ΔV_2 , respectively, the expression

$$E_{\text{int}} = -\frac{15d}{8\pi\gamma^2} \Delta V_1 \Delta V_2 \frac{\Gamma}{r^3}. \quad (3)$$

d is a function of the elastic constants and is negative for metals; $\gamma = 3(1-\sigma)/(1+\sigma)$ with σ = Poisson's ratio; $\Gamma = 0.400 - 2(l^2m^2 + m^2n^2 + n^2l^2)$ with l, m, n the direction cosines with respect to the cubic axes of the vector connecting the defects; and r is the distance between the defects. Since the sign of ΔV_{int} is opposite to that of ΔV_{vac} , we have $E_{\text{int}} \propto -\Gamma/r^3$. Now $\Gamma(100) = 0.40$, $\Gamma(110) = -0.10$, and $\Gamma(111) = -0.27$, so we see there is a cone about the $[100]$ direction in which E_{int} is attractive. Values of Γ/r^3 are tabulated in Table II. Using the 10°K values for the elastic constants of copper and the limiting estimates of Tewordt for the volume change appropriate to the interstitial and the vacancy, we have evaluated the interaction energy in Eq. (3). Subtracting the interaction energy from the migration energy of the free interstitial (0.12 eV) which we obtain in the following paper, gives the energy of recombination E_{rec} . These results are given in Table II. Using the E_{rec} values to order the substages, and assuming that I_A is the first stable close pair, i.e., there are not close-pair peaks below 14°K, we associate

TABLE II. Interaction energy and energy of recombination. N designates the lattice site. Γ and r are taken from Table I. E_{int} is the interaction energy calculated from Eq. (3). $E_{\text{rec}} = 0.12 - E_{\text{int}}$. The E_{rec} (obs.) are the text E_A, E_B, E_C values. All energies are expressed in electron volts.

N	(Γ/r^3)	E_{int}	E_{rec}	E_{rec} (obs)
4A	1.48×10^{-2}	0.13	-0.01	0.05
7A	4.15×10^{-3}	0.0365	+0.084	0.085
10A	3.20×10^{-3}	0.028	+0.0920	0.095
5	2.36×10^{-3}	0.021	+0.099	
11A	1.84×10^{-3}	0.016	+0.104	
12A	1.04×10^{-3}	0.009	+0.111	
9	1.87×10^{-4}	0.002	+0.118	

¹⁵ L. Tewordt, Phys. Rev. **109**, 61 (1958).

¹⁶ J. D. Eshelby, Acta Met. **3**, 487 (1955).

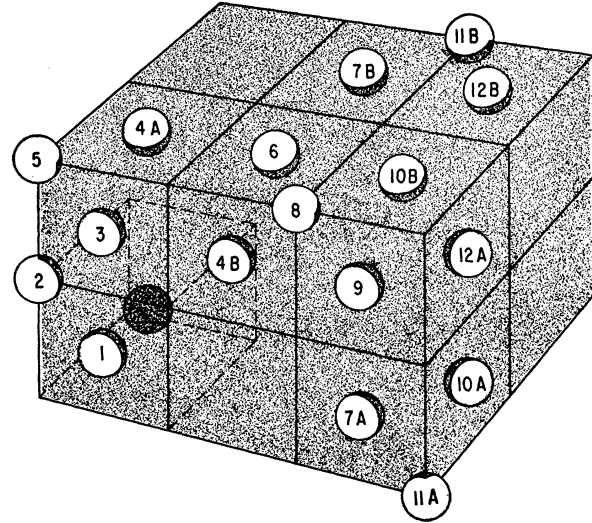


FIG. 10. The face-centered cubic copper lattice with a body-centered interstitial (dark atom) in lower left unit cell. The atom sites are numbered with increasing distance from the interstitial. Only crystallographically nonequivalent atoms are shown.

site 4 with I_A , site 7A with I_B and site 10A with I_C . Clearly this treatment is not adequate.

Certainly the use of elasticity theory at these close spacings is not justified, and the marked preference for vacancies sites in a $[100]$ direction is probably unrealistic. Further, important factors, such as the change in the electronic energy, have been omitted. If we neglect theory completely and look for a natural group of three sites to correspond to the observed three substages, we note that there is a distinct gap in distance between the sites 4, 5, 6 and the sites 7, 8, 9. Possibly then I_A corresponds to 4, I_B to 5, and I_C to 6 with the vacancy at site 7 sufficiently removed to be essentially free. An alternative approach would be to assume that the amount of recovery associated with a given recovery peak is proportional to the number of equivalent vacancy sites of the corresponding close pair species. This is the same as assuming that the partitioning among the close pair species was governed by a random process. From this approach, we would conclude that I_A is associated with site 2, I_B with site 4 and I_C with site 5.

Clearly at this point we must conclude that a final decision on the question of the defect configuration corresponding to the substages must await further calculation and experiment.

ACKNOWLEDGMENTS

The authors gratefully acknowledge the contribution of Dr. M. D. Fiske to their work. The help of Mrs. E. Fontanella, Mr. L. B. Nesbitt, Dr. T. I. Moran, Dr. W. F. Westendorp, and Dr. J. W. Cahn in the conduct of the experiments and analysis is also gratefully acknowledged.